doi:10.1038/nature09677

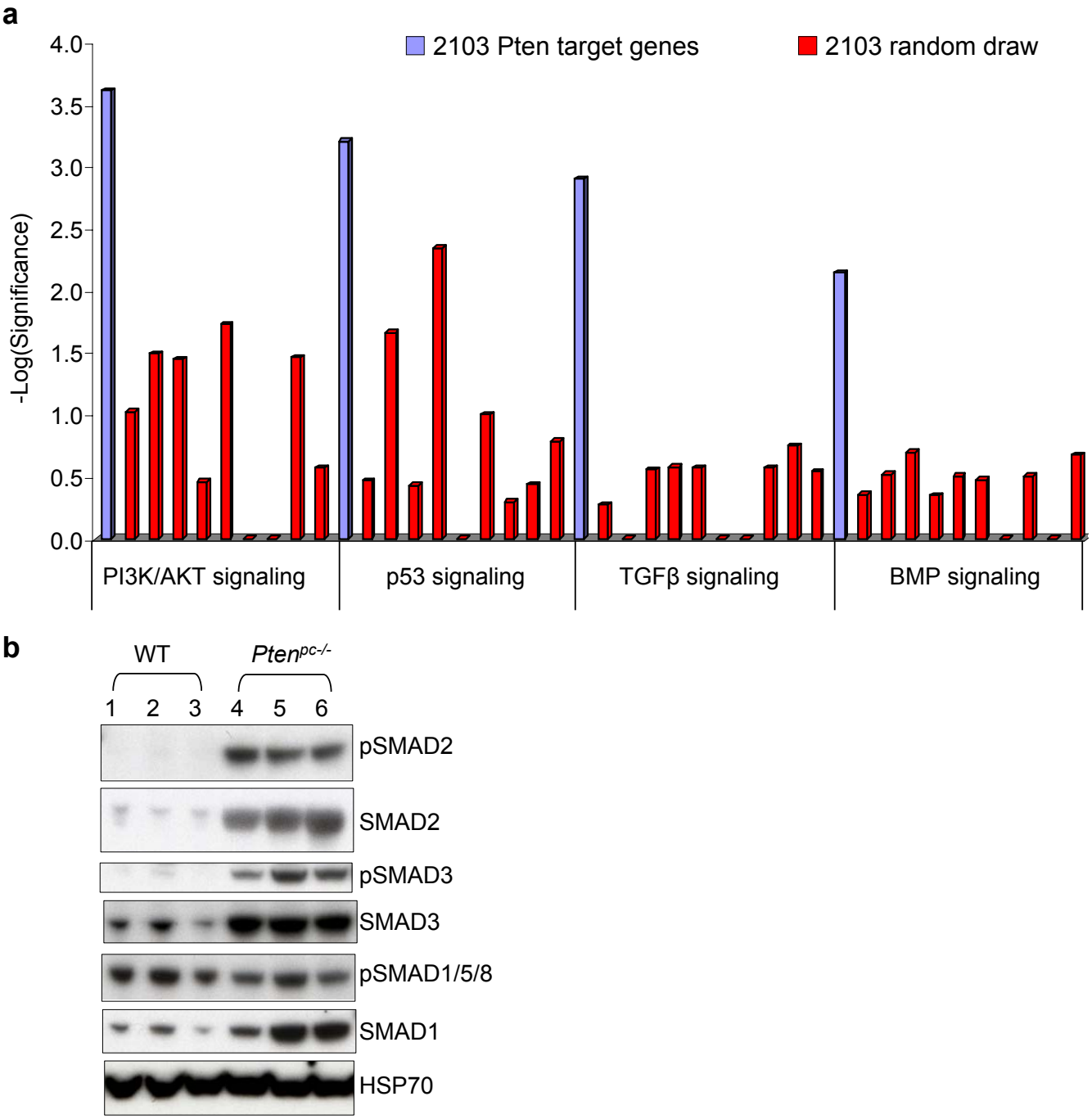

Supplementary Fig. S1. Ingenuity knowledge-based pathway analysis (IPA) for Canonical Pathways. a, *Pten*$^{pc-/-}$ anterior prostate tumors show significant activation of PI3K, p53, TGFβ and BMP signaling pathways by Ingenuity knowledge-based canonical pathway analysis of 2103 differentially expressed genes between WT and *Pten*$^{pc-/-}$ anterior prostate (in blue) compared to 10 randomly drawn gene sets of equal size (in red). **b,** Biochemical studies confirmed marked activation of the TGFβ/BMP signaling surrogates in poorly progressive *Pten*$^{pc-/-}$ prostate tumors. Western blot analysis of AP tissues from each genotype at 15 weeks shows pSMAD2, SMAD2, pSMAD3, SMAD3, and SMAD1 upregulation in *Pten*$^{pc-/-}$ mice compared to AP tissues from control mice. HSP70 serves as the sample loading control.

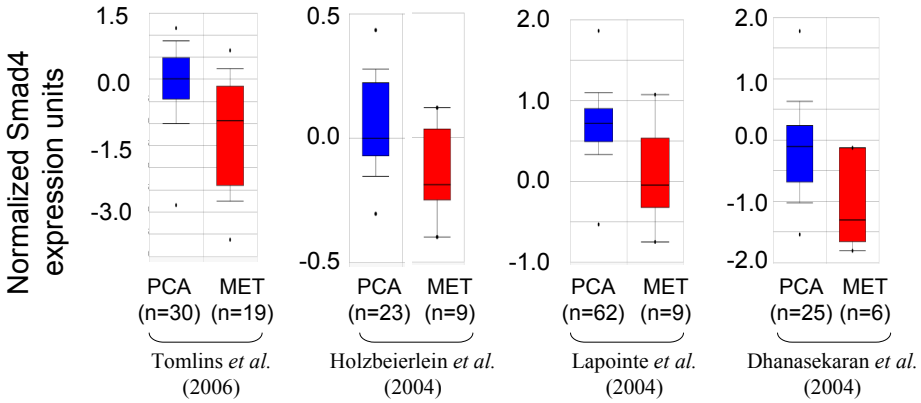

Supplementary Fig. S2. Oncomine boxed plot of SMAD4 expression levels between human primary prostate cancer (PCA) and metastasis (MET) in multiple datasets including Tomlins *et al.* (2006)[34], Holzbeierlein *et al.* (2004)[35], Lapointe *et al.* (2004)[36], and Dhanasekaran *et al.* (2004)[37].

References:

34. Tomlins,S.A. *et al.* Integrative molecular concept modeling of prostate cancer progression. *Nat. Genet.* **39**, 41-51 (2007).

35. Holzbeierlein,J. *et al.* Gene expression analysis of human prostate carcinoma during hormonal therapy identifies androgen-responsive genes and mechanisms of therapy resistance. *Am. J. Pathol.* **164**, 217-227 (2004).

36. Lapointe,J. *et al.* Gene expression profiling identifies clinically relevant subtypes of prostate cancer. *Proc. Natl. Acad. Sci. U. S. A* **101**, 811-816 (2004).

37. Dhanasekaran,S.M. *et al.* Molecular profiling of human prostate tissues: insights into gene expression patterns of prostate development during puberty. *FASEB J.* **19**, 243-245 (2005).

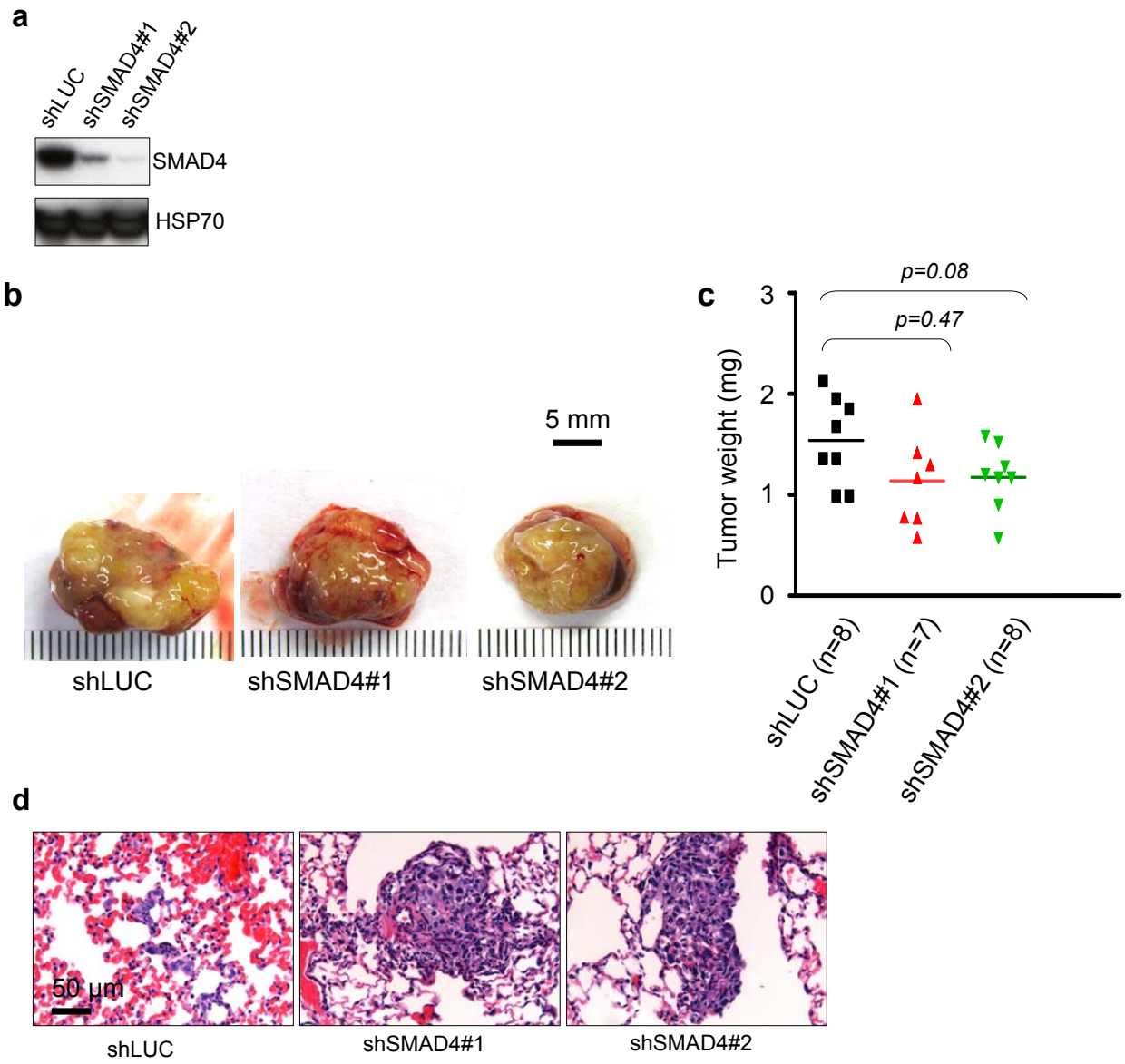

Supplementary Fig. S3. Biological impact of shRNA-mediated knockdown of human *SMAD4* in human PC3 prostate cancer cells. a, Western blot analysis of SMAD4 following shRNA-mediated knockdown of SMAD4 in human PCA PC3 cells. **b,** Implanted control (shLUC) or stably SMAD4 depleted (shSMAD4#1 and #2) PC3 cells implanted under the kidney capsule of immunocompromised mice formed primary tumors with comparable size *in vivo*. Shown are the gross anatomical presentations of representative shLUC, shSMAD4#1 and #2 kidney implantation tumors at 7 weeks. **c,** Quantification of the weight of kidney implantation tumors at 7 weeks. **d,** H&E-stained sections of representative lung fields with metastatic foci at 7 weeks following implantation of PC3 cells in the kidney capsule of immunocompromised nude mice.

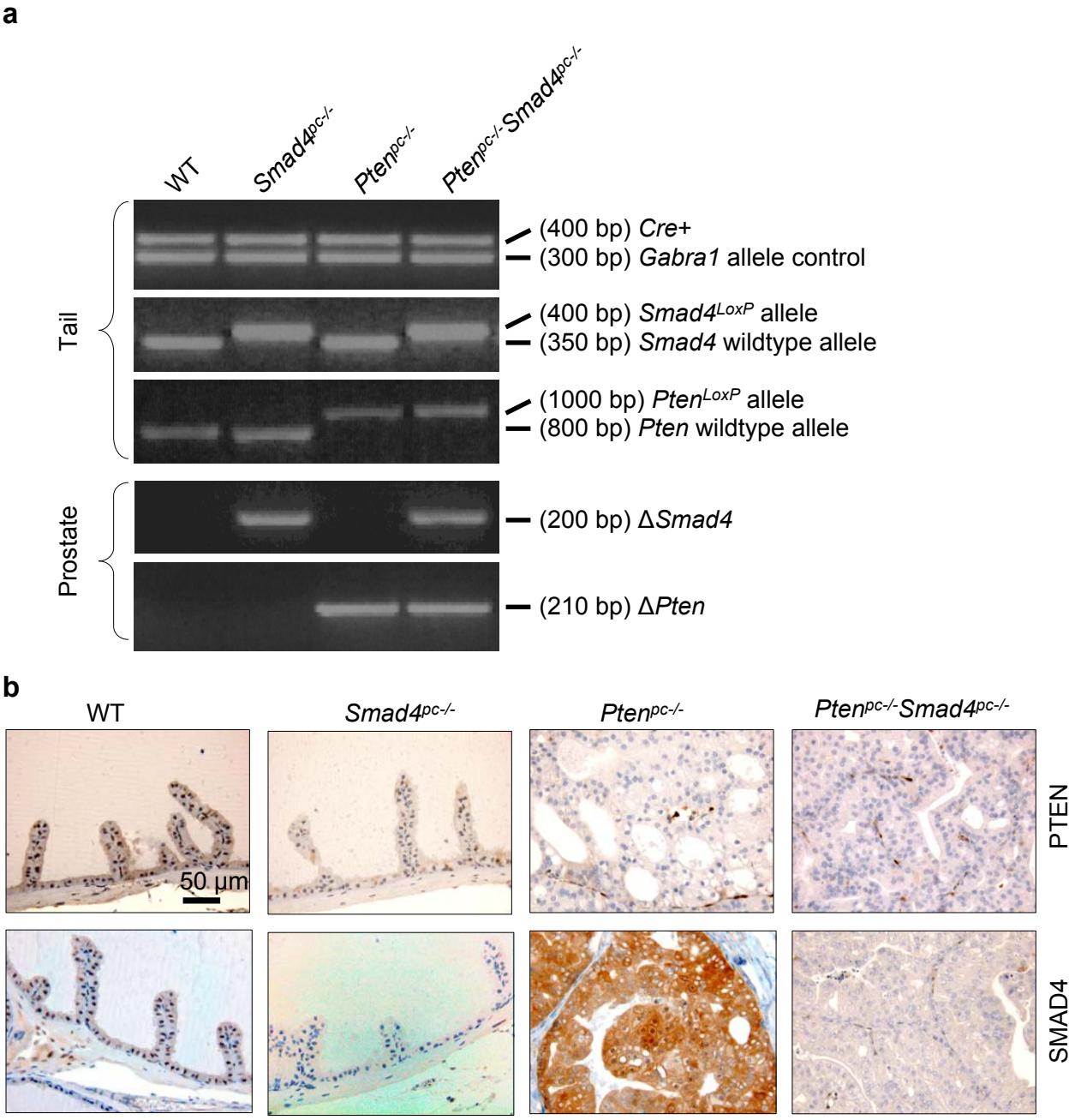

Supplementary Fig. S4. Immunohistochemical confirmation of efficient Cre-mediated deletion of *Pten* and *Smad4* conditional alleles in *Pten*$^{pc-/-}$*Smad4*$^{pc-/-}$ mouse model. a, PCR-based identification of mutants from non-recombined and recombined allelic combinations of *Smad4*^{loxP} and *Pten*^{loxP} alleles prior to Cre-mediated recombination on tail DNA, or after Cre-mediated recombination on prostate DNA. **b,** Immunohistochemical analyses of Pten expression levels showed efficient deletion PTEN in both in *Pten*$^{pc-/-}$ and *Pten*$^{pc-/-}$*Smad4*$^{pc-/-}$ mouse model. Notably, immunohistochemical analysis shows enhanced expression of SMAD4 in *Pten*$^{pc-/-}$ and efficient loss of Smad4 expression in *Pten*$^{pc-/-}$*Smad4*$^{pc-/-}$ mouse model.

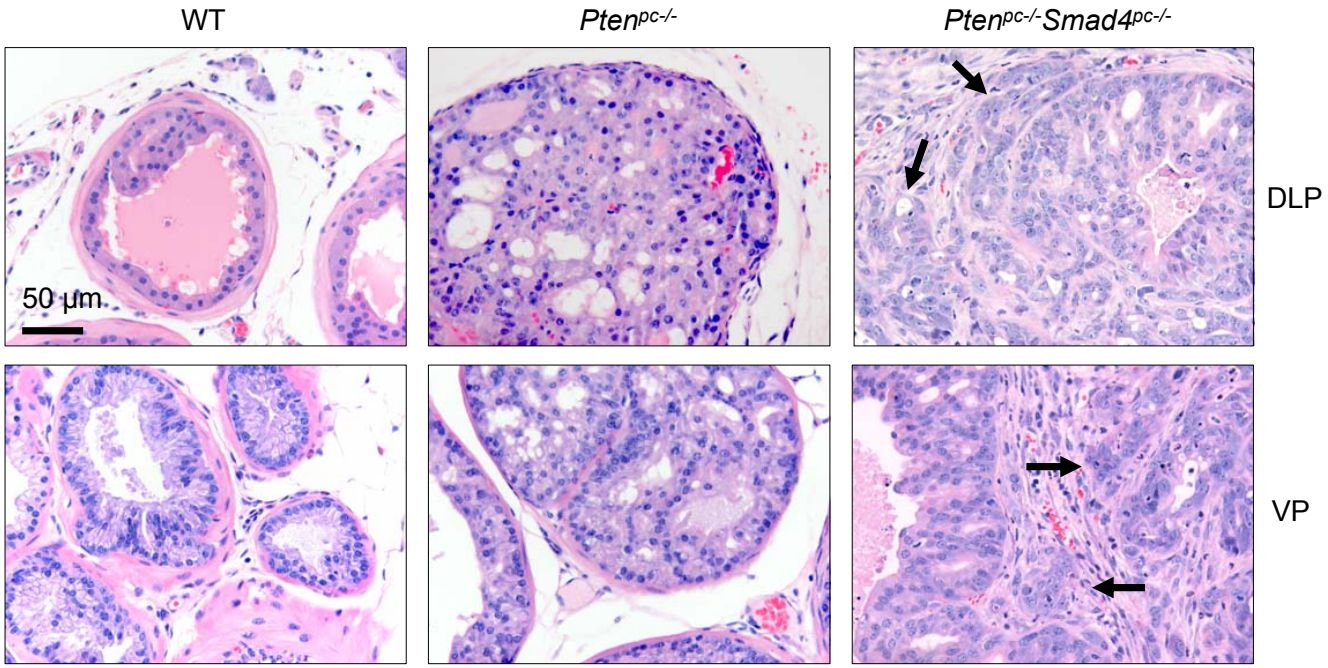

Supplementary Fig. S5. *Smad4* deletion drives progression of *Pten*$^{pc-/-}$ prostate tumors to invasive PCA by 15 weeks of age in all prostate lobes. Analysis of H&E-stained section of dorsolateral prostate (DLP) and ventral prostate (VP) in WT, *Pten*$^{pc-/-}$, and *Pten*$^{pc-/-}$*Smad4*$^{pc-/-}$ prostates at 15 weeks of age reveals invasive PCA in *Pten*$^{pc-/-}$*Smad4*$^{pc-/-}$ DLP (arrow) and VP (arrow).

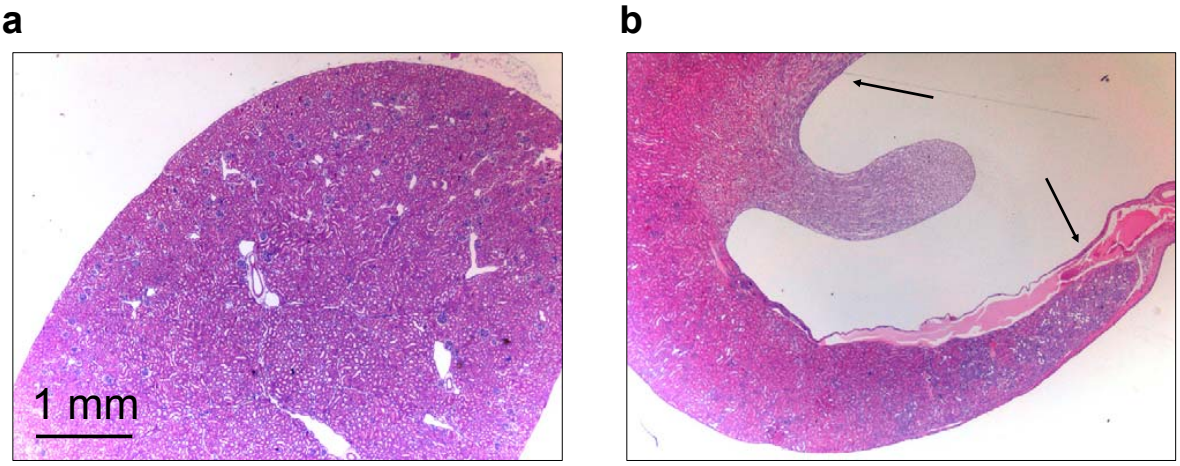

Supplementary Fig. S6. Histopathological presentation of hydronephrosis in *Pten*$^{pc-/-}$*Smad4*$^{pc-/-}$ mice. a, b, Representative H&E-stained kidney sections from *Pten*$^{pc-/-}$ mice (**a**) and *Pten*$^{pc-/-}$*Smad4*$^{pc-/-}$ (**b**) mice reveals hydronephrosis (arrow) in the latter.

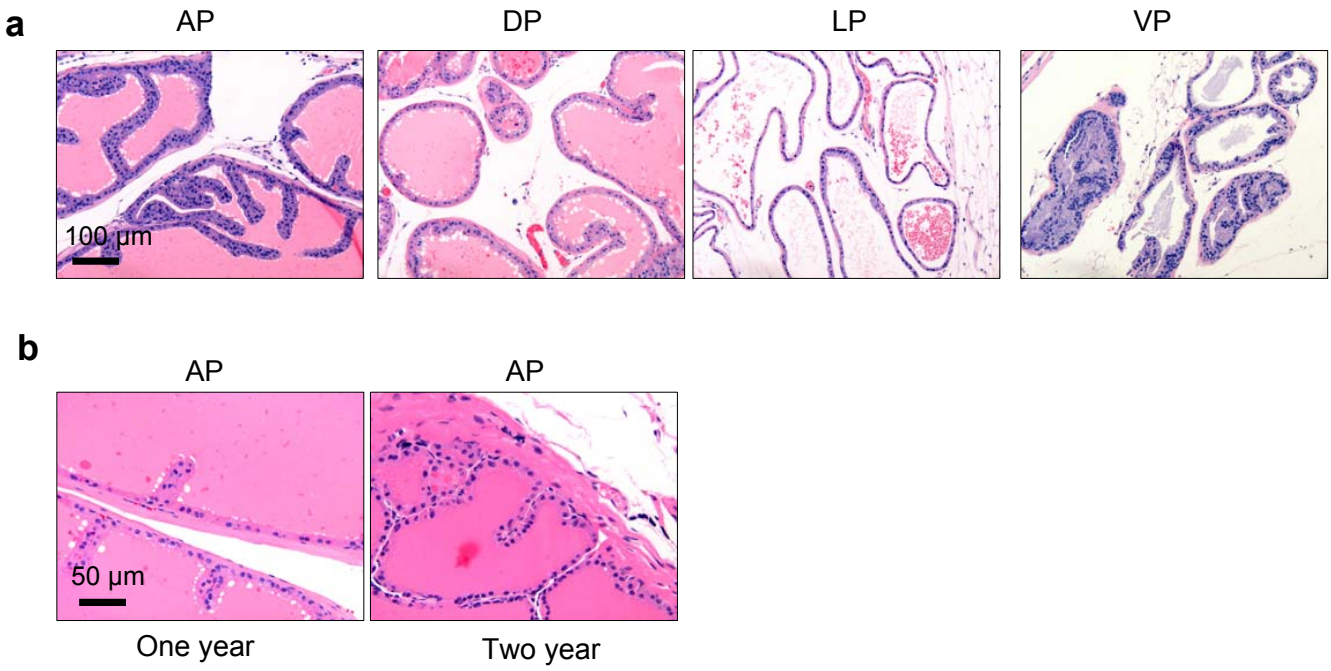

Supplementary Fig. S7. Loss of *Smad4* does not provoke prostate neoplasia. a, H&E-stained sections of anterior prostate (AP), dorsal prostate (DP), lateral prostate (LP), and ventral prostate (VP) in *Smad4*$^{pc-/-}$ mouse at 15 weeks of age show normal prostate structure. **b,** Deletion of *Smad4* does not alter prostate histology as shown in H&E-stained sections of AP at one and two years of age in *Smad4*$^{pc-/-}$ mice.

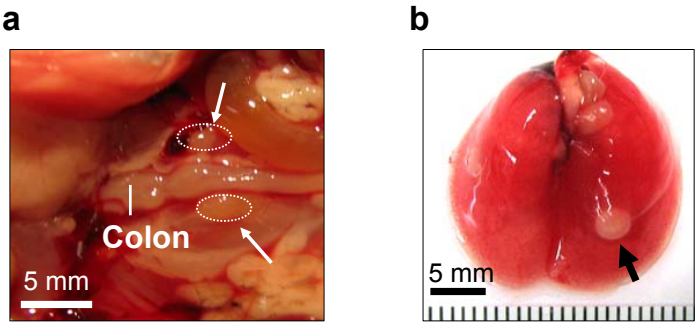

Supplementary Fig. S8. *Smad4* deletion drives progression of *Pten*-deficient prostate tumor to highly aggressive prostate cancer metastatic to lymph node and lung. a, b, Gross anatomy of representative lumbar lymph nodes (dashed circle) (**a**) and lung with metastatic foci (arrow) (**b**).

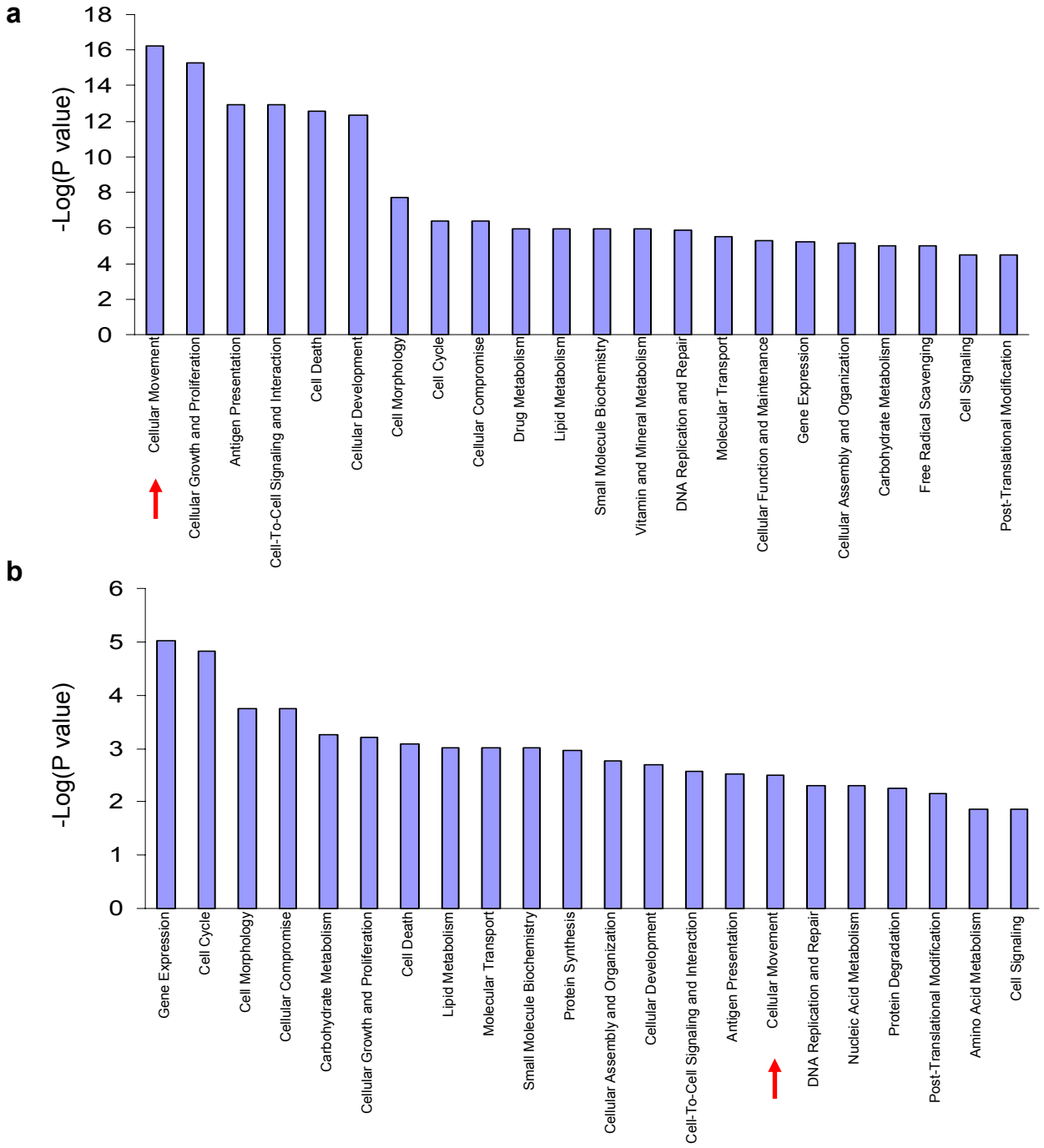

Supplementary Fig. S9. Ingenuity knowledge-based molecular and cellular functions analysis of the *Pten*$^{pc-/-}$*Smad4*$^{pc-/-}$ tumor transcriptome shows significant enrichment of cell movement genes. a, Ingenuity knowledge-based molecular and cellular functions analysis (IPA) of the 267 genes differentially expressed between *Pten*$^{pc-/-}$ and *Pten*$^{pc-/-}$*Smad4*$^{pc-/-}$ anterior prostate tumors in 15 week old mice showed a significant enrichment of genes as indicated. The most significantly enriched gene-categories is "Cellular Movement" (rank #1, p=6.17x10^{-17}) (arrow). **b,** IPA of the 243 genes differentially expressed between *Pten*$^{pc-/-}$ and *Pten*$^{pc-/-}$*p53*$^{pc-/-}$ anterior prostate tumors reveals that those genes have potential roles as indicated. In contrast to the *Pten*$^{pc-/-}$*Smad4*$^{pc-/-}$ tumors, the IPA of *Pten*$^{pc-/-}$*p53*$^{pc-/-}$ tumors show that cell movement genes rank #16 (P=0.00313) (arrow).

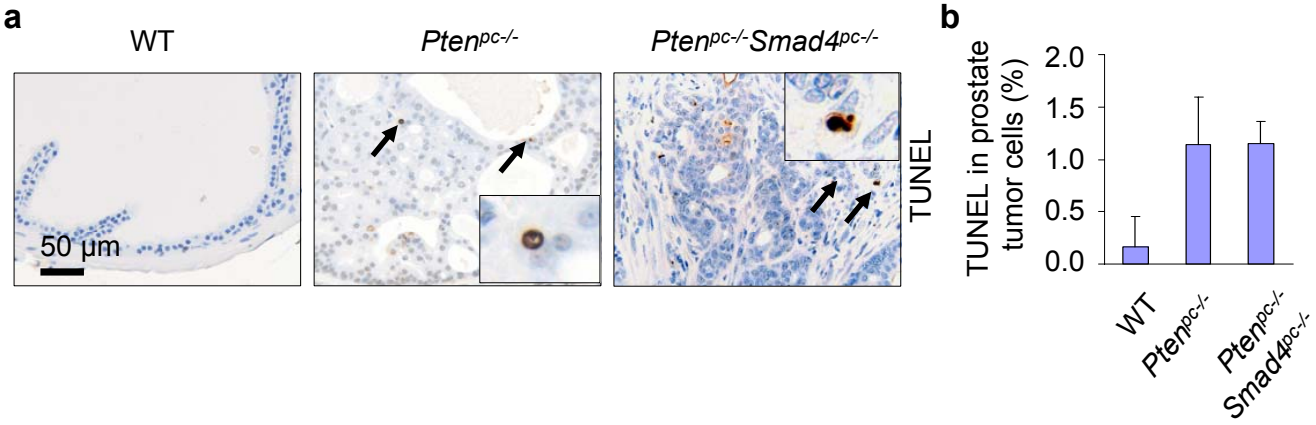

Supplementary Fig. S10. TUNEL analysis shows no significant difference in *Pten*$^{pc-/-}$*Smad4*$^{pc-/-}$ and *Pten*$^{pc-/-}$ prostate tumors. a, Representative pictures of TUNEL analysis of anterior prostate tumors from *Pten*$^{pc-/-}$*Smad4*$^{pc-/-}$ (inserted picture is 4 times enlarged) and *Pten*$^{pc-/-}$ mice aged 15 weeks (inserted picture is 4 times enlarged). **b,** Quantification of TUNEL assay. Multiple sections from three mice of each genotype were counted TUNEL-positive cells. Error bars in (b) represent s.d. for a representative experiment performed in triplicate.

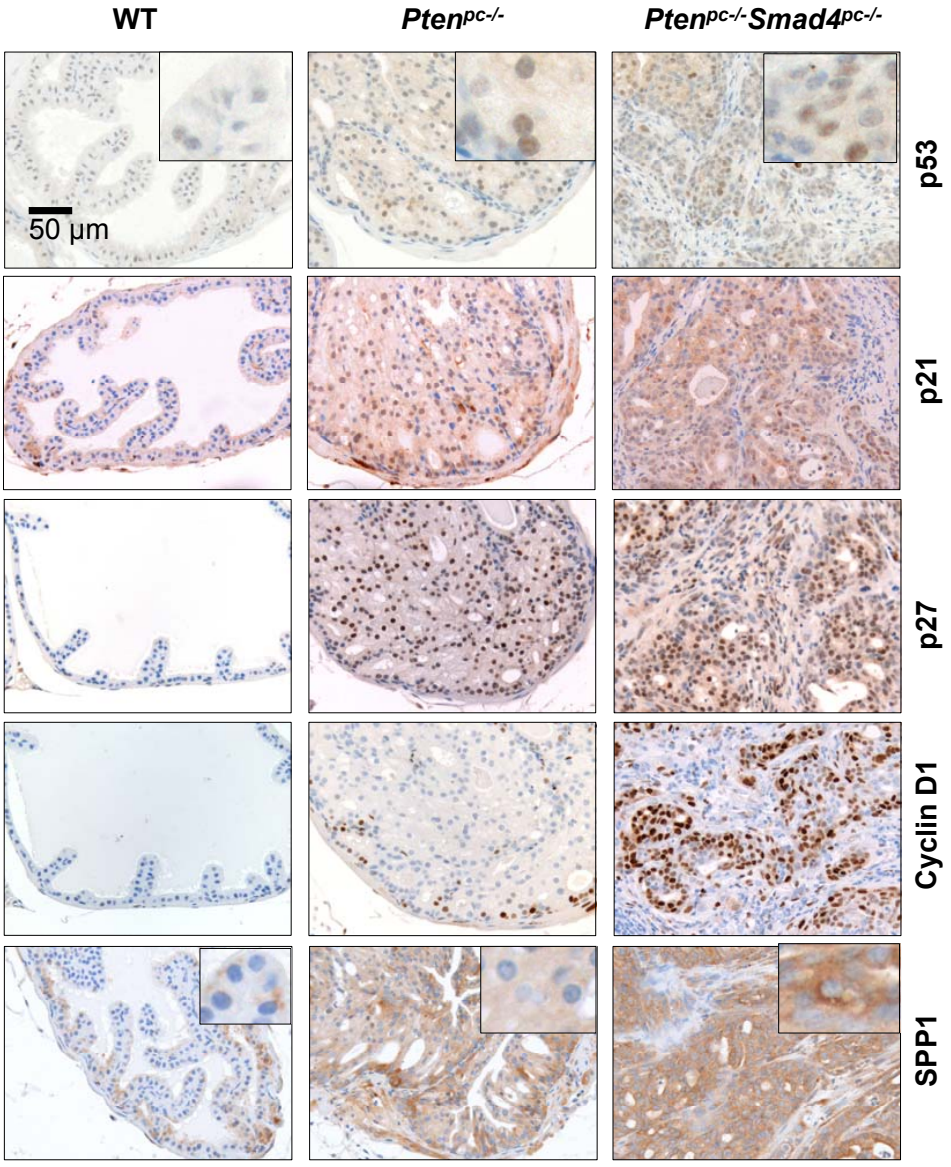

Supplementary Fig. S11. Immunohistochemical analyses of p53, p21, p27, Cyclin D1, and SPP1 reveals enhanced expression of Cyclin D1 and SPP1 in *Pten*$^{pc-/-}$*Smad4*$^{pc-/-}$ compared to *Pten*$^{pc-/-}$ samples. p53, p21, and p27 expression levels show no significant differences between *Pten*$^{pc-/-}$ and *Pten*$^{pc-/-}$*Smad4*$^{pc-/-}$ samples. Cyclin D1 and SPP1 expression levels are markedly increased in *Pten*$^{pc-/-}$ *Smad4*$^{pc-/-}$ relative to *Pten*$^{pc-/-}$ samples (inserted picture is 4 times enlarged).

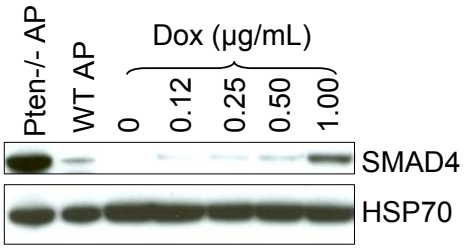

Supplementary Fig. S12. Establishment of inducible *Pten*$^{pc-/-}$*Smad4*$^{pc-/-}$ SMAD4-TetOn cells. *Pten*$^{pc-/-}$*Smad4*$^{pc-/-}$ SMAD4-TetOn cells were induced to express SMAD4 using doxycycline (Dox) for 24 hours. Western blot analysis shows SMAD4 induction upon adding Dox. HSP70 serves as the sample loading control.

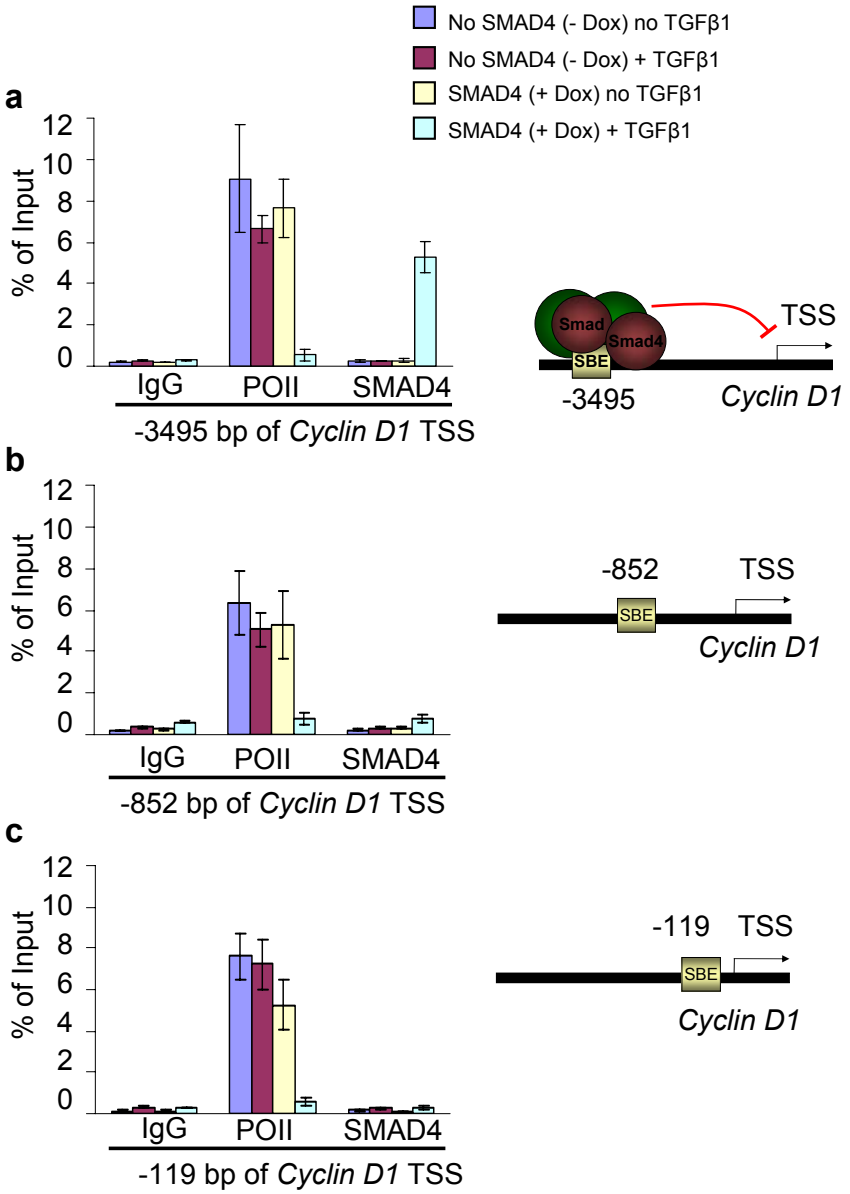

Supplementary Fig. S13. The *Cyclin D1* promoter is occupied by SMAD4 in SMAD4-induced TGFβ1-stimulated *Pten*$^{pc-/-}$*Smad4*$^{pc-/-}$ SMAD4-TetOn cells. a, The *Cyclin D1* promoter spanning SBE at -3495 is occupied by SMAD4 in SMAD4-induced (upon adding 1μg/mL doxycycline for 24 hours pretreatment) TGFβ1-stimulated (adding 0.5 ng/mL TGFβ1) *Pten*$^{pc-/-}$*Smad4*$^{pc-/-}$ SMAD4 TetOn cells. **b,c,** The *Cyclin D1* promoter spanning SBE at -852 (**b**) or -119 (**c**) is not occupied by SMAD4 in these cells. On the schematic representation of the *Cyclin D1* promoter, SMAD4 binding sites are depicted relative to the +1 transcriptional start site (TSS). Primers were designed to encompass the SMAD binding sites. Quantification of ChIP analysis on promoter was assessed by qPCR analysis. Error bars in (b-d) represent s.d. for a representative experiment performed in triplicate. Normal mouse IgG and Anti-RNA Polymerase II (POII) serve negative and positive controls, respectively.

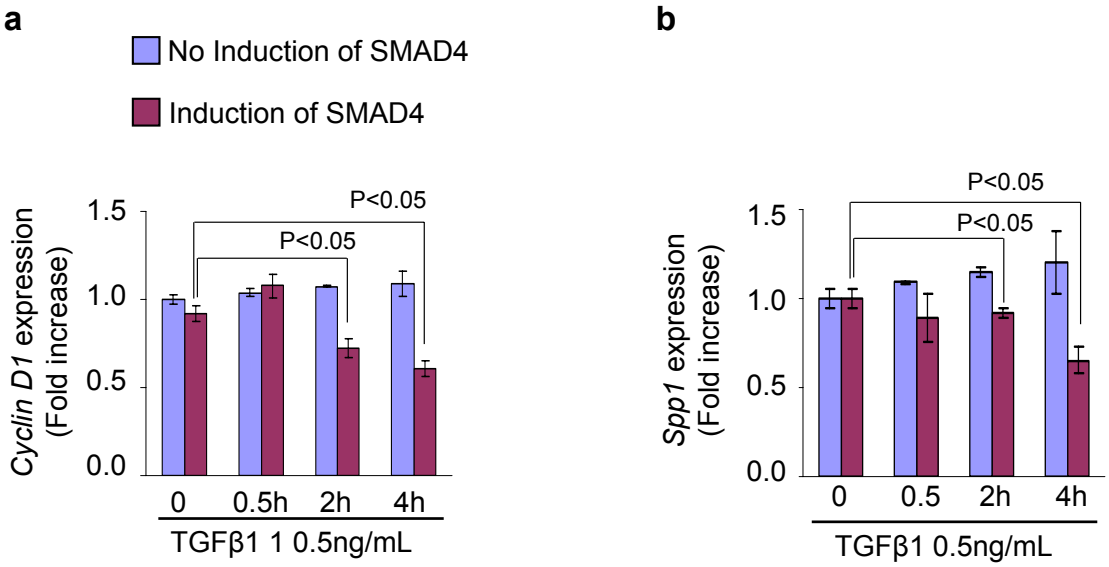

Supplementary Fig. S14. SMAD4 suppresses *Cyclin D1* and *Spp1* mRNA expression upon TGFβ1 treatment. a, b, Expression of *Cyclin D1* mRNA (**a**) and *Spp1* mRNA (**b**) in SMAD4-induced (upon adding 1μg/mL doxycycline for 24 hours pretreatment) TGFβ1-stimulated SMAD4-TetOn versus SMAD4-not induced TGFβ1-stimulated SMAD4-TetOn cells. Cells were treated with 0.5 ng/mL TGFβ1 at the indicated time points and *Cyclin D1* and *Spp1* mRNA expression was measured by RT-qPCR. Error bars in (a-b) represent s.d. for a representative experiment performed in triplicate.

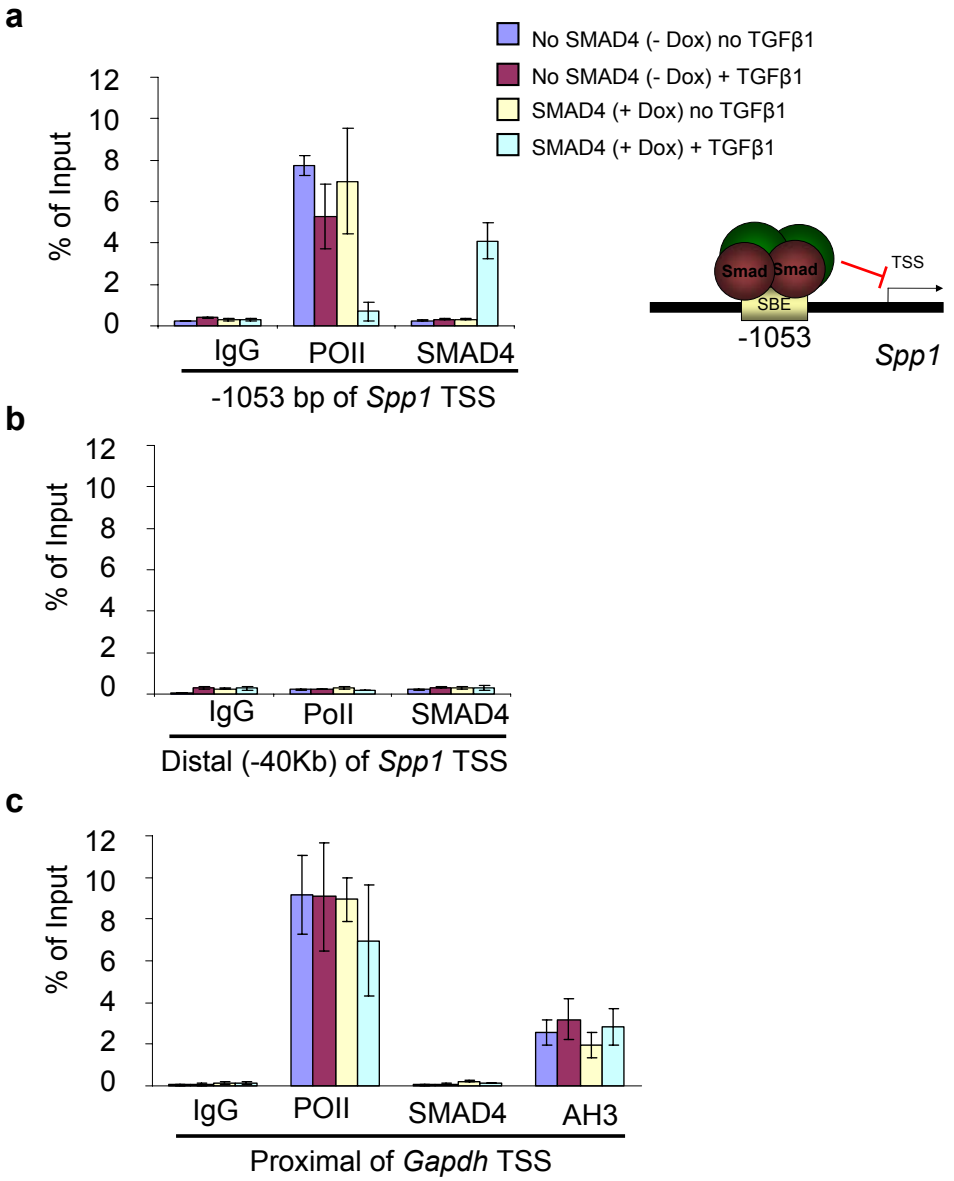

Supplementary Fig. S15. The *Spp1* promoter is occupied by SMAD4 in SMAD4-induced TGFβ1-stimulated *Pten*$^{pc-/-}$*Smad4*$^{pc-/-}$ SMAD4-TetOn cells. a, b, The *Spp1* promoter spanning SBE at -1053bp is occupied by SMAD4 (**a**) but not at random sequence around -40kb (**b**) in SMAD4-induced (upon adding 1μg/mL doxycycline for 24 hours pretreatment) TGFβ1-stimulated *Pten*$^{pc-/-}$*Smad4*$^{pc-/-}$ SMAD4 TetOn cells. On the schematic representation of the *Spp1* promoter, SMAD4 binding sites are depicted relative to the +1 TSS. Primers were designed to encompass the SBE at -1053bp or encompass a random sequence around distal -40kb relative to the +1 *Spp1* TSS. Quantification of ChIP analysis on promoter was assessed by qPCR analysis. Error bars represent s.d. for a representative experiment performed in triplicate. **c,** The house keeping gene *Gapdh* proximal promoter region around the TSS is enriched for the acetyl-Histone H3 (AH3) and POII, but not occupied by SMAD4 in *Pten*$^{pc-/-}$*Smad4*$^{pc-/-}$ SMAD4 TetOn cells. Quantification of ChIP analysis on promoter was assessed by qPCR analysis. Error bars represent s.d. for a representative experiment performed in triplicate.

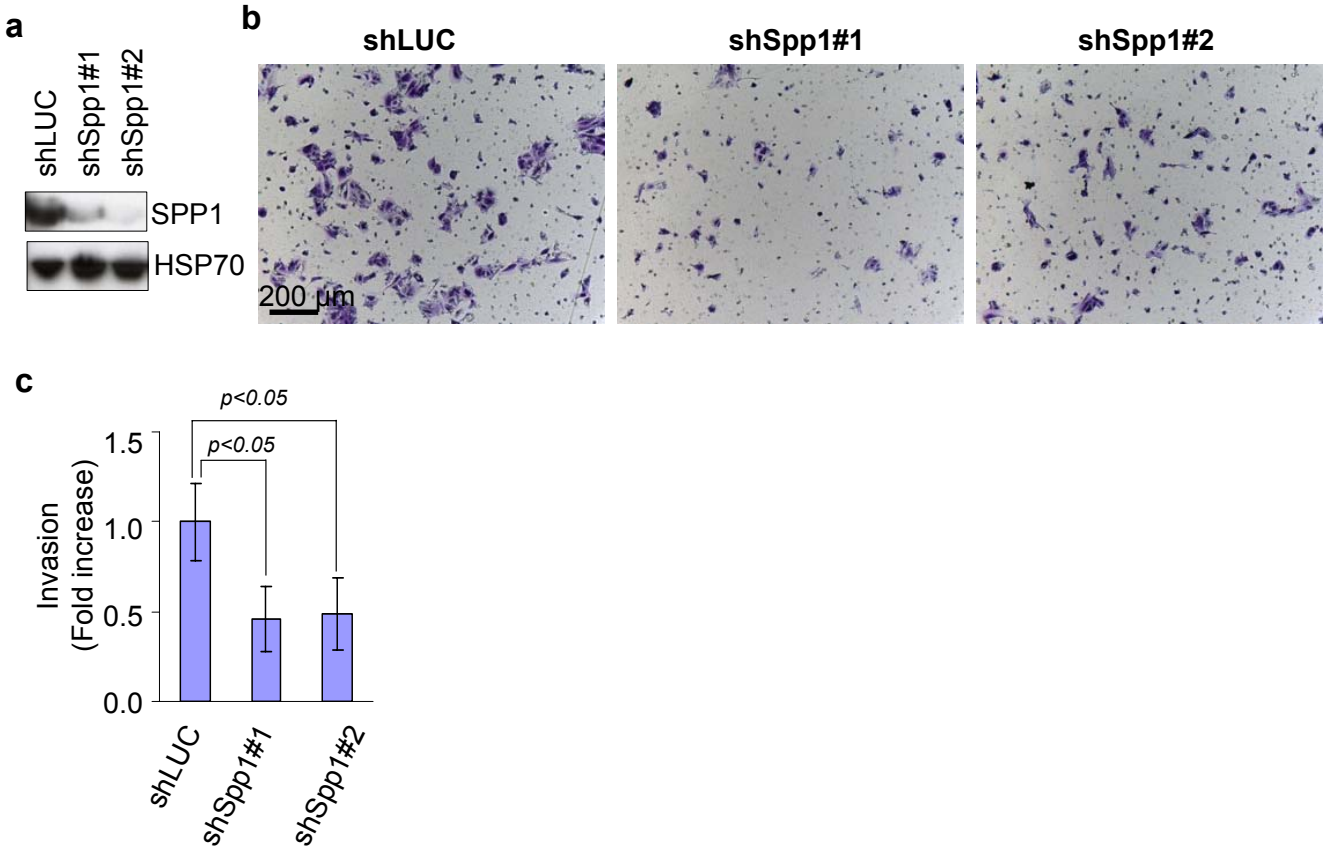

Supplementary Fig. S16. shRNA-mediated knockdown of SPP1 in *Pten*$^{pc-/-}$*Smad4*$^{pc-/-}$ tumor cells inhibits cell invasion in the Boyden chamber assay. a, Western blot analysis shows effective knockdown of SPP1 in mouse *Pten*$^{pc-/-}$*Smad4*$^{pc-/-}$ double mutants cell line. HSP70 serves as the sample loading control. **b,** Representative images of invasion assay showing shLUC control and two independent shSpp1 hairpins. **c,** Knockdown of *Spp1* significantly inhibits invasive activity of mouse prostate tumor cells isolated from *Pten*$^{pc-/-}$*Smad4*$^{pc-/-}$ double mutants by invasion assay. Error bars represent s.d. for a representative experiment performed in triplicate.

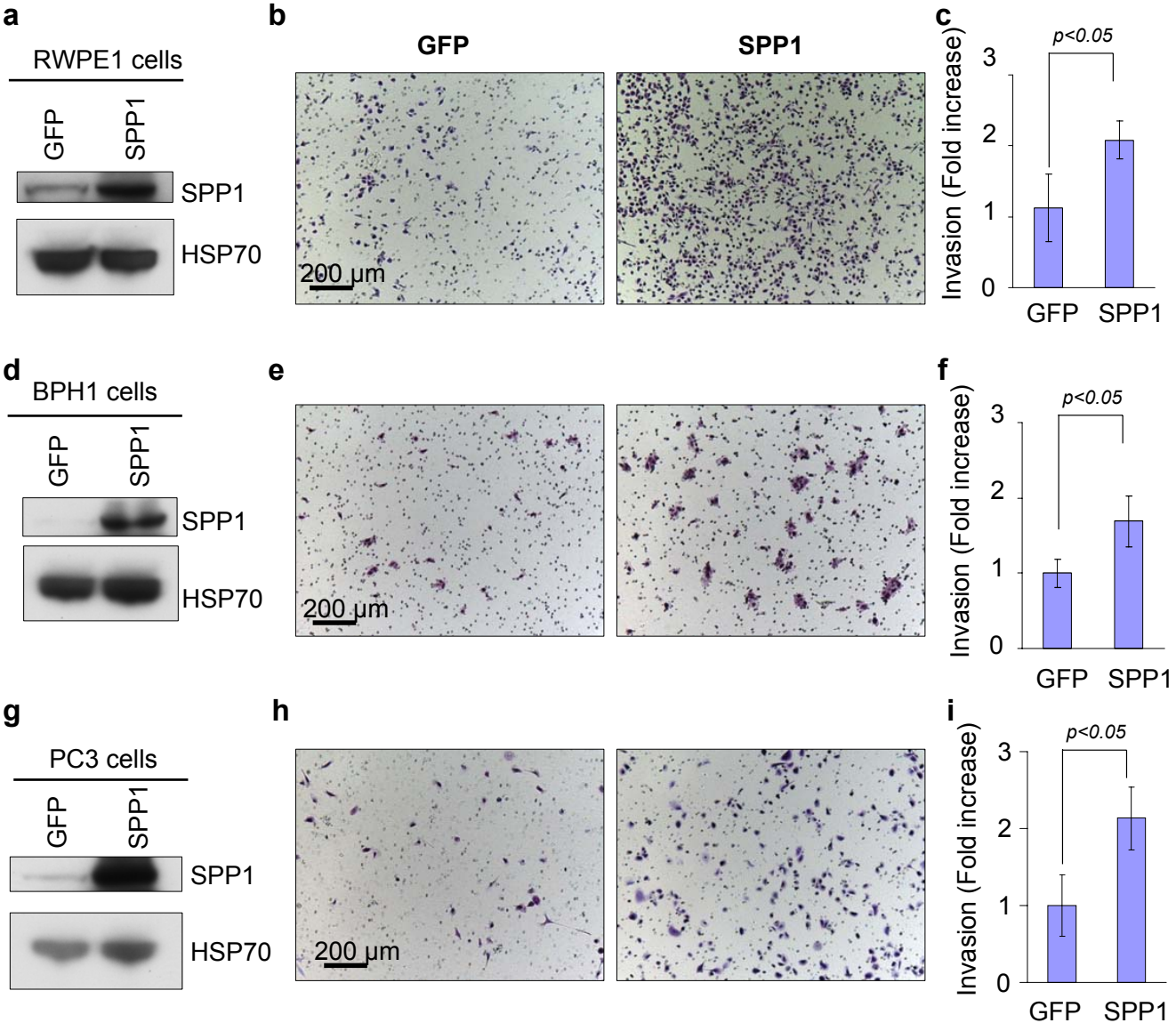

Supplementary Fig. S17. Enforced expression of SPP1 enhances invasive activity of multiple human prostate cancer cells in the Boyden chamber assay. Western blot analysis shows elevated expression of SPP1 in SPP1-transduced RWPE1 (**a**), BPH1 (**d**), and PC3 prostate cells (**g**). Hsp70 serves as the sample loading control. Representative images of invasion assay of SPP1- versus GFP-transduced RWPE1 (**b**), BPH1 (**e**), and PC3 prostate cells (**h**). Quantification of invasion assay with RWPE1 (**c**), BPH1 (**f**), and PC3 human prostate cell (**i**). Error bars represent s.d. for a representative experiment performed in triplicate.

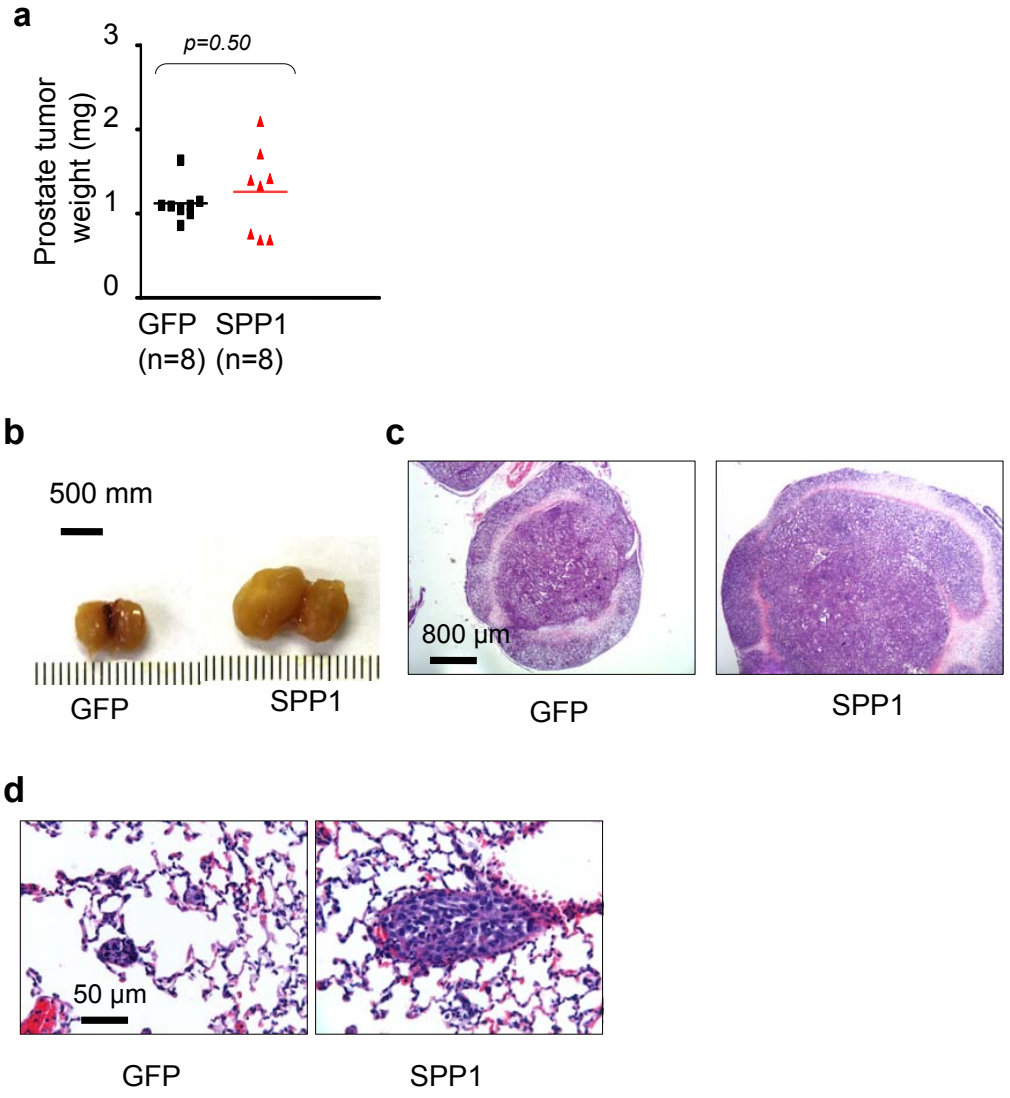

Supplementary Fig. S18. Enforced SPP1 expression significantly increases metastatic activity of PC3 cells from orthotopic xenograft to lumbar lymph nodes and to lung. **a,** Enforced SPP1 expression has no significant impact on primary orthotopic xenograft tumor growth of PC3 cells. **b,** Gross anatomy of representative GFP and SPP1 lumbar lymph nodes at 8 weeks following implantation. **c,** H&E stained sections of representative GFP and SPP1 lumbar lymph nodes at 8 weeks following implantation. **d,** H&E-stained sections of representative lung fields with metastatic foci at 8 weeks following implantation of PC3 cells in the prostate of immunocompromised nude mice.

a **Step 1: Adding one proliferation readout gene from the 267 gene list to the PTEN/SMAD4 two gene signature:**

The selection criteria are:
(1) implicated in tumor cell proliferation/cell cycle regulation
(2) positively with PCA progression in at least one PCA progression datasets in Oncomine
(3) with putative Smad binding sites

Models		Coeff of the 3th marker	Wald P value of the 3th marker	P value of the combined model scores
PTEN + SMAD4				0.496
PTEN + SMAD4 +	CCND1	0.634	0.238	0.172

b **Step 2: Adding one invasion readout gene from the 267 gene list to the three gene signature:**

The selection criteria are:
(1) implicated in tumor cell movement
(2) positively with PCA progression in at least one PCA progression datasets in Oncomine
(3) with putative Smad binding sites

Models		Coeff of the 4th marker	Wald P value of the 4th marker	P value of the combined model scores
PTEN + SMAD4				0.496
PTEN + SMAD4 + CCND1				0.172
PTEN + SMAD4 + CCND1+	SPP1	0.936	0.0080	0.0028
PTEN + SMAD4 + CCND1+	ID1	-0.434	0.229	0.071

c **Step 3: Validating the 4-gene signature of Pten/Smad4/Cyclin D1/SPP1 in independent datasets**:

Validating at mRNA level:
(1) the PHS mRNA expression-cohort (n=116; lethal metastasis as outcome)

Validating at protein level:
(2) the TMA of PHS cohort (n=405; lethal metastasis as outcome)
(3) the TMA of Director's Challenge cohort (n=40; BCR as outcome).

(1) Models with PHS RNA expression profiling data (lethal cases, n=30; indolent cases, n=86)	**(2) Models with PHS TMA** (lethal cases, n=38; indolent cases, n=367)	**(3) Models with Directors Challenge TMA** (Recurrent cases, n=18; indolent cases, n=22)
Model 1. Gleason only: C=0.70 (95% CI = 0.63-0.76)	Model 1. Gleason only: C=0.774 (95% CI = 0.70-0.84)	Model 1. Gleason only: C=0.704, (95% CI = 0.31-0.91)
Model 2. 4-genes only: C=0.716 (95% CI = 0.67-0.84)	Model 2. 4-protein only: C=0.829 (95% CI = 0.76-0.91)	Model 2. 4-genes only: C=0.691 (95% CI = 0.41-0.88)
Model 3. Gleason + 4 genes: C=0.816 (95% CI = 0.75-0.90)	Model 3. Gleason + 4 genes: C=0.882 (95% CI = 0.82-0.94)	Model 3. Gleason + 4 genes: C=0.740 (95% CI = 0.46-0.91

Supplementary Fig. S19. Derivation of 4-gene signature for prognosis. Although genetically proven to predispose the mouse to develop metastatic PCA, the initiating events of Pten/Smad4 do not by themselves prognosticate risk for BCR (p=0.496) in the Glinsky cohort. To enhance the prognostic value of these two events, additional markers from the 267 differentially expressed genes in the *Pten$^{pc-/-}$Smad4$^{pc-/-}$* signature (Supplementary Data 2) were selected computationally to reflect the two salient biological features of proliferation and invasion in the metastatic *Pten$^{pc-/-}$Smad4$^{pc-/-}$* PCAs using the Glinsky et al cohort as a training set. **a,** For the marker reflecting proliferation, the selection criteria are: (i) implicated in tumor cell proliferation/cell cycle regulation, (ii) positive association with PCA progression in at least one PCA dataset in Oncomine, and (iii) containing putative Smad binding sites (SBE) in their promoters (Supplementary Data 2). Cyclin D1 was the only gene that fit the criteria. **b,** To select the marker for tumor cell invasion, the selection criteria are: (i) genes linked to "Cellular Movement" among the 267 differentially expressed genes the *Ptenpc-/-Smad4pc-/-* signature and functionally validated to promote invasion of PC3 cells *in vitro*, (ii) positive association with PCA progression in at least one PCA dataset in Oncomine, and (iii) containing putative Smad binding sites (SBE) in their promoters (Supplementary Table 1). Both SPP1 and ID1 fulfilled the criteria. Next, multivariate Cox regression modeling showed that SPP1 when modeled with Pten/Smad4/Cyclin D1 provided significant prediction for BCR risk (p=0.0028) while ID1 did not. **c,** Prognostic significance of this 4-marker signature was tested in independent datasets at both RNA level and protein levels in comparison with Gleason Score alone or in combination using C-Statistics (see Full methods).

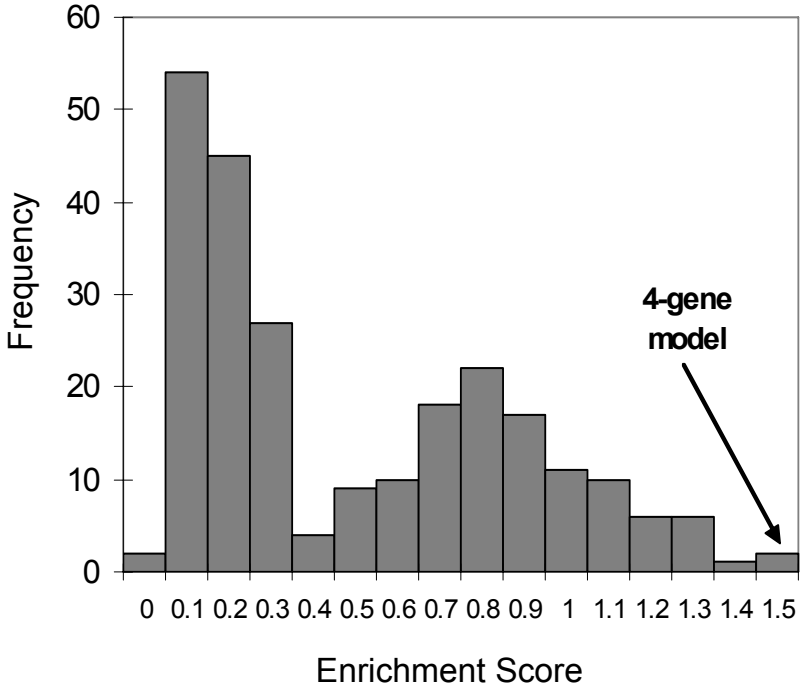

Supplementary Fig. S20 . The 4-gene set of PTEN/SMAD4/Cyclin D1/SPP1 ranked as the most enriched among 244 bidirectional signatures curated in the MSigDB (version 2.5) by gene-set-enrichment testing in predicting metastatic lethal outcome.

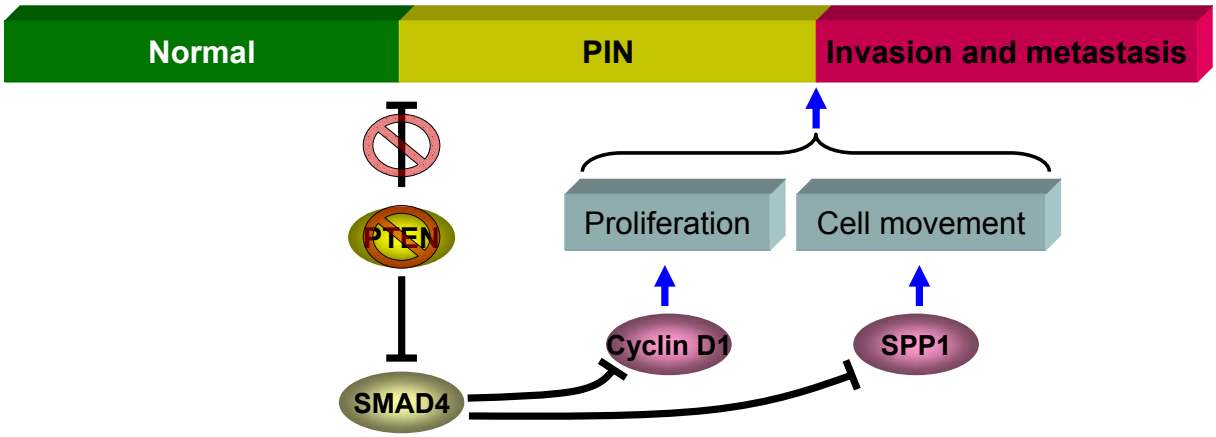

Supplementary Fig. S21. A model of the role of SMAD4 in constraining progression of PTEN deficient prostate neoplasms. PTEN inactivation in normal prostate of the mouse lead to development of PIN. PTEN inactivation results in a robust increase in expression of Smad4, which in turn suppress key cell proliferation mediator Cyclin D1 and key cell movement mediator SPP1. Concomitant Pten and Smad4 inactivation in the mouse prostate epitheliam can activate the expression Cyclin D1 and SPP1, and enhance tumor cell proliferation and drive invasion to a invasive and metastatic PCA phenotype.

Supplementary Table 1. The frequency of metastasis of each genotype.

	Metastasis			
Age (Weeks)	**WT**	***Smad4*$^{pc-/-}$**	***Pten*$^{pc-/-}$**	***Pten*$^{pc-/-}$ *Smad4*$^{pc-/-}$**
7-15	0/5	0/5	0/5	0/5
16-35	0/5	0/5	0/10	*25/25 to lymph nodes, 3/25 to lung, 0/25 to bone
36-55	0/5	0/5	0/10	None alive
55-110	0/5	0/5	1/8 to lymph nodes, 1/8 to lung, 0/8 to bone	None alive

*Metastatic foci in lumbar lymph nodes and/or lungs in the *Pten*$^{pc-/-}$*Smad4*$^{pc-/-}$ mice aged 16-35 weeks (n=25) show significant (P<0.0001, asterisk)difference from in *Pten*$^{pc-/-}$ (n=20).

Supplementary Table 2. cDNAs in "Cell Movement" functional category assayed for ability to enhance invasion of human prostate cell lines. Superscript a,b,c,d in the column of Gene Name see foot note.

Gene Name	Invasion fold change in PC3 cells (p<0.05)	Invasion fold change in RWPE1 cells (p<0.05)	Invasion fold change in BPH1 cells (p<0.05)	Human cDNA clones
Up-regulated gene list (15 genes):				
SPP1 [a,b,d]	3.3	2	1.7	Human ORFeome Internal ID 7415
FSCN1 [a,b]	3.1	3	NA	Human ORFeome Internal ID 4674
KRT6A [a,b]	6.5	NA	NA	Human ORFeome Internal ID 4870
LOX [b,d]	2.6	2.7	NA	Requested as FLJ92566AAAF from NITE
SLPI [b,d]	2.22	2.6	NA	Human ORFeome Internal ID13088
ITGAX [b,d]	Not Hit	NA	NA	Human ORFeome Internal ID 10181
CD44 [b]	2.4	2.4	NA	Human ORFeome Internal ID 4311
CD53 [b]	1.8	2.7	NA	Human ORFeome Internal ID 11381
LGALS1 [b]	3.3	3.6	NA	Human ORFeome Internal ID 6097
FSTL1 [b]	Not Hit	NA	NA	Human ORFeome Internal ID 3529
GJA1 [b]	Not Hit	NA	NA	Human ORFeome Internal ID 1142
IL4R [b]	Not Hit	NA	NA	Requested as FLJ95762AAAF from NITE
MSN [b]	Not Hit	NA	NA	Human ORFeome Internal ID 7789
TGFBI [b]	Not Hit	NA	NA	Human ORFeome Internal ID 3543
TIMP1 [b]	Not Hit	NA	NA	Human ORFeome Internal ID 5734
Down-regulated gene list 6 genes):				
ID1 [a,b,d]	0.2	Not Hit	NA	Human ORFeome Internal ID 604
NCOA4 [a,b,d]	Not Hit	NA	NA	Human ORFeome Internal ID 2434
STAT5A [a,b]	Not Hit	NA	NA	Human ORFeome Internal ID 8201
TFF3 [a,b]	Not Hit	NA	NA	Human ORFeome Internal ID 12996
ID3 [b,d]	Not Hit	NA	NA	Human ORFeome Internal ID 3761
CTSE [b]	0.5	Not Hit	NA	Human ORFeome Internal ID 11112

[a] Human PCA progression correlated gene (P<0.0001) from Oncomine (http://www.oncomine.org/) PCA progression datasets, including:

1. Yu,Y.P. et al. Gene expression alterations in prostate cancer predicting tumor aggression and preceding development of malignancy. J. Clin. Oncol. 22, 2790-2799 (2004).
2. Dhanasekaran,S.M. et al. Delineation of prognostic biomarkers in prostate cancer. Nature 412, 822-826 (2001).
3. Tomlins,S.A. et al. Integrative molecular concept modeling of prostate cancer progression. Nat. Genet. 39, 41-51 (2007).
4. Holzbeierlein,J. et al. Gene expression analysis of human prostate carcinoma during hormonal therapy identifies androgen-responsive genes and mechanisms of therapy resistance. Am. J. Pathol. 164, 217-227 (2004).
5. Lapointe,J. et al. Gene expression profiling identifies clinically relevant subtypes of prostate cancer. Proc. Natl. Acad. Sci. U. S. A 101, 811-816 (2004).
6. Dhanasekaran,S.M. et al. Molecular profiling of human prostate tissues: insights into gene expression patterns of prostate development during puberty. FASEB J. 19, 243-245 (2005).

[b] "Cell movement" functional category from IPA analysis.

[c] Cell cycle regulators (KEGG: http://www.broadinstitute.org/gsea/msigdb/geneset_page.jsp?geneSetName=HSA04110_CELL_CYCLE&keywords=cell%20cycle).

[d] Containing putative Smad binding sites (SBE) in the promoter

Supplementary Table 3. Clinical characteristics of the Glinsky cohort.

	Glinsky GEP
N	79
BCR cancers, N (%)	29 (37%)
Duration of follow-up	0.12 – 8.8 years
Mean (SD) age at diagnosis, years	61 (6) years
Mean (SD) pre-RP PSA, ng/ml	11.2 (9.2)
TNM Stage, %	
T1	41.8%
T2	53.2%
T3	2.5%
N1	3.8%
Gleason grade, %	
2-6	21.5%
3+4	38.0%
4+3	17.7%
8-10	22.8%

Supplementary Table 4. Univariate Cox proportional hazard analysis with individual signature genes on the 79 PCA patients from the Glinsky cohort.

Gene	**Coefficient**	**Hazard Ratio**	**P value**
PTEN	0.006	1.01	0.99
SMAD4	-0.442	0.64	0.50
CCND1	0.658	1.93	0.22
SPP1	0.781	2.18	0.017

Supplementary Table 5. Multivariate Cox proportional hazard analysis with all 4 signature genes on the Glinsky cohort. Linear combination of the expression of 4 genes corresponds to log-rank test P value = 0.0025 in association with BCR, and overall C index = 0.66.

Gene	Coefficient	Hazard Ratio	P value
PTEN	0.094	1.10	0.80
SMAD4	-0.157	0.85	0.81
CCND1	1.068	2.91	0.067
SPP1	0.936	2.55	0.008

Supplementary Table 6. Clinical characteristics of the Physicians' Health Study participants in the TMA and gene expression profiling cohorts.

	Physicians' Health Study	
	TMA	**GEP**
N	405	116
Years of diagnosis	1983-2004	
Lethal cancers, N	38	30
Year of follow-up for mortality/metastases	2009	2007
Mean (SD) age at diagnosis, years	66 (6) years	67 (7) years
TNM Stage, %		
T1/2	77%	65%
T3/T4	20%	26%
N1	4%	9%
Gleason grade, N (%)		
2-6	27%	11%
3+4	36%	31%
4+3	19%	28%
8-10	18%	30%
Mean body mass index at diagnosis, kg/m^2	25.4	25.4
Race, % Caucasian	95%	95%

Supplementary Table 7. C-statistics (and 95% CI) of lethal prostate cancer comparing models with the clinical information and the 4-protein signature in the Physicians' Health Study (N=405 men). Gleason score and age at diagnosis are modeled as a continuous variable; TNM stage is modeled as a binary variable as T1/T2 vs. T3/T4/N1.

Model	C-statistics (95% CI)
Model 1. Gleason score	0.773 (0.688-0.857)
Model 2. Gleason, age at diagnosis, TNM stage	0.842 (0.762-0.922)
Model 3. 4-gene signature	0.827 (0.749-0.905)
Model 4. 4-genes + Gleason grade	0.876 (0.810-0.942)
Model 5. 4-genes + Gleason, age at dx, TNM stage	0.913 (0.863-0.962)

Supplementary Table 8. Summary of clinical characteristics of 40 high quality core samples in the Directors Challenge TMA cohort.

	Directors Challenge TMA
N	40
BCR cancers, N (%)	18 (45%)
Duration of follow-up	0.1 – 12.3 years
Mean (SD) age at diagnosis, years	59 (6) years
TNM Stage, %	
T2	52.5%
T3/T4	47.5%
Gleason grade, %	
2-6	32.5%
3+4	40%
4+3	15%
8-10	12.5%